

A kinetic model for iron aluminide coating by low pressure chemical vapor deposition: Part II. Model formulation

J.T. John^a, G.B. Kale^a, S.R. Bharadwaj^b, R.S. Srinivasa^c, P.K. De^{a,*}

^aMaterials Science Division, Bhabha Atomic Research Centre, Trombay, Mumbai 400 085, India

^bApplied Chemistry Division, Bhabha Atomic Research Centre, Trombay, Mumbai, India

^cDepartment of Metallurgical Engineering and Materials Science, Indian Institute of Technology Bombay, Powai, Mumbai, India

Abstract

Formation of aluminide diffusion coatings on iron, nickel and cobalt by pack cementation and chemical vapor deposition (CVD) involves a series of similar steps, the slowest among them are the transport of aluminum bearing species from the vapor phase to the substrate by gas-phase diffusion and the solid-phase diffusion of aluminum into the substrate to form the aluminide phases. The former increases the surface concentration of aluminum in the coating while the latter decreases it. Modeling of the process is based on the observation that the surface composition of the coating tends to reach a steady state value in a short time after the commencement of the process, at which stage the rates of the above two processes are equal. However, in the case of iron aluminide coatings produced by low pressure chemical vapor deposition (1.33 ± 0.13 kPa), the rate of transport of aluminum to the substrate is much faster than the solid phase diffusion of aluminum into the iron substrate since the diffusion coefficients of the vapor species are inversely proportional to pressure and the diffusion layer thickness is reduced considerably at low pressures. Under this condition, the vapor transport is no longer a rate-determining step and the composition of the aluminide coating is decided by the kinetics of the solid phase diffusion. This model could explain the kinetics of the process, surface composition and concentration profile of the coating.

Keywords: Coatings; Aluminizing; Diffusion; Chemical vapor deposition

1. Introduction

Iron aluminide coatings are applied on steels to improve their corrosion resistance in oxidizing, sulphidizing and carburizing environments encountered in coal gasification plants, crude oil refineries and petrochemical industries. These coatings are produced by the diffusion of aluminum into the surface of a component by solid, liquid and vapor processes. However, high quality coatings of uniform thickness and composition are produced more often by vapor processes such as pack cementation and chemical vapor deposition (CVD). Modeling work attempts to rationalize the coating characteristics, such as thickness and composition for a given set of experimental parameters. The coating process is divided into a number of steps and each step is analyzed to find out its impact on the

coating process and model is the cumulative effect of all such steps correlated to coating characteristics. The important steps involved in the formation of aluminide coatings by CVD are similar to those of the pack cementation process. They are:

- (i) Formation of the aluminum subchlorides by the reaction of the aluminum metal or alloy and the aluminum chloride vapor. In pack cementation the subchlorides are formed by the reaction of activators and the aluminum metal or alloy added to the pack.
- (ii) Transport of the subchlorides to the substrate by gas-phase diffusion.
- (iii) Reaction leading to the deposition of aluminum at the substrate surface.
- (iv) Diffusion of aluminum into substrate with the formation of the coating consisting of different intermetallic phases.
- (v) Diffusion of the reaction products from the substrate back to the reactor.

It is believed that chemical reactions in steps (i) and (iii) are very fast at the operating temperature and the kinetics of the coating process is controlled by step (ii), the vapor transport and step (iv), the solid-phase diffusion. Step (v) is important as it decides the purity of the coating.

Since hydrogen cannot reduce AlCl_3 to aluminum due to unfavorable free energy values ($\Delta G_{1173}^0 \approx +217 \text{ kJ mol}^{-1}$), the aluminide coating is produced from the subchlorides of aluminum step i, which are produced by the reaction between pure aluminum or an aluminum alloy and aluminum chloride (or aluminum and the activators in the case of pack cementation). The deposition reaction can be represented schematically by the equation:



The forward reaction takes place in the CVD reactor and the reverse reaction at the substrate.

An analysis of the kinetic and thermodynamic processes involved in pack cementation (steps i and ii) was reported by Levine and Caves [1]. They calculated the partial pressures of aluminum subhalides that would be formed at the operating temperature in the bulk pack and at the surface of the substrate. Diffusion of aluminum-bearing species to the substrate takes place because of the difference in the activity (partial pressure) of aluminum subhalides in the reactor and those at the surface of the aluminide coating. In pack cementation, as the aluminum from the layers adjacent to the sample is transported to the substrate, an aluminum depleted zone is formed close to the substrate, whose thickness increases with the duration of deposition. Assuming that all the aluminum transported as subchlorides to the substrate is deposited, they derived an expression for the rate of transport of aluminum to the substrate, which obeyed a parabolic rate law. The weight gain, thus calculated matched well with the experimental results [1].

The intermetallic phase formed at the surface and its composition and thickness are more important parameters that decide the utility of the coating than the coating weight. Hickl and Heckel [2] reported a mathematical treatment of the diffusion process for the nickel aluminide coatings produced by pack cementation, which could predict the coating thickness and the surface composition. Later this was extended to iron aluminide coatings [3]. They assumed a two-step pack aluminizing process involving initial influx of aluminum in a high activity pack where a Ni_2Al_3 (δ) phase was formed and a subsequent partial homogenization under zero influx of aluminum, where, the required phase, NiAl (β) was produced at the surface. The coating layer thickness was studied over a wide range of temperature and time and found that the layer growth followed parabolic kinetics. Using that data, the average interdiffusion coefficients of nickel and aluminum were calculated in β and δ phases (NiAl and Ni_2Al_3 , respectively). Assuming that the diffusion coefficients did not change with composition, they set up differential equations for the layer growth and calculated concentration profiles.

Initially when the coating was produced in a high-activity aluminum pack, 97% of the coating consisted of the δ phase (Ni_2Al_3). By heat treatment at the same temperature, the δ phase was transformed to the β phase (NiAl), whose thickness and concentration profile were calculated.

The assumption that the diffusion coefficient is independent of composition will introduce significant error in the concentration profiles of coatings produced in a low activity pack. In this case, only the NiAl phase is formed, in which the interdiffusion coefficient varies by approximately three orders of magnitude. When the coatings contain predominantly δ phase, the error will be low as variation of interdiffusion coefficient with composition is not high. However, when the β phase is formed by heat treatment, the assumption can introduce appreciable error. Hence, Sarkhel and Seigle [4], in their model for the formation of aluminide coating on nickel by pack cementation, expressed the interdiffusion coefficient as an exponential function of composition. They calculated the rate of movement of the phase boundaries in the coating including the outward movement of the surface as a result of the aluminum pickup. The multi-layer diffusion equation for the nickel–aluminum system was then solved by an analytical method to obtain the concentration profiles for various aluminum activities in the pack. They obtained the concentration profiles that were more realistic than that of the Hickl and Heckel model for low-activity packs [4].

By combining this model and the transport of aluminum from the pack by gas-phase diffusion (Levine and Caves' model) [1], a more complete model that could predict the rate of the coating formation, the surface composition of the coating layer and the concentration profile was developed for aluminide coating on nickel by pack cementation [5–10]. According to this new model, the composition of the surface of the coating was decided by the dynamic equilibrium between the transport of aluminum from the pack to the substrate by gas-phase diffusion and that from the surface into the substrate by solid phase diffusion. It was shown that the aluminum concentration at the surface reaches a constant value shortly after the commencement of the deposition [6]. At the steady state both the rates will be equal. The rate of transport of aluminum from the pack to the coating surface decreased with increase in aluminum content at surface and the rate of diffusion of aluminum from the surface into the sample increased with increase in aluminum content at surface. Hence, a plot of the two rates against surface composition will intersect at a point where the rates are equal and this point will uniquely define the surface composition and rate of formation of the coating. Nciri and Vandenbulke [11–13] applied this model for the iron aluminide coatings by pack cementation and obtained excellent correlation between the theoretical and experimental values of surface composition.

The model, which was developed for pack cementation process, was extended with suitable modifications for chemical vapor deposition at atmospheric pressure (APCVD) of aluminide coatings on nickel and nickel base alloys [14–16]. According to Sun et al. [14], the difference

between pack cementation and CVD arises from the kinetics of the gaseous transport. In CVD, the mass transport by gaseous diffusion is a linear function of time since, the diffusion layer is of constant width and the diffusion of aluminum in solid phase will be a parabolic function of time. Hence, to equate the mass transport from the mobile phase to the substrate by gas-phase diffusion and from the surface into the substrate by solid phase diffusion, they used the relationship,

$$W^2 = k_g^2 t^2 = k_s t \quad (2)$$

where k_g is the rate of mass transport by gaseous diffusion in CVD, k_s is the rate of mass transport by solid state diffusion and, t is the duration of deposition.

Hence, in CVD modeling they plotted $k_g^2 t$ (instead of k_g) and k_s as function of surface concentration of aluminum. Further, in the case of pack cementation, the diffusion layer thickness could be expressed as a function of coating weight and the pack aluminum content, which leads to the parabolic kinetics [1]. In CVD, the diffusion layer thickness is constant and since it was not possible to find a simple relationship between diffusion layer thickness and experimental parameters, they assumed an arbitrary value of 1 cm [14]. They could explain the metallurgical phases formed on the surface by this model.

2. This work

The aluminide coating process by low-pressure chemical vapor deposition (LPCVD) was described in the first part of this paper [17]. Aluminum chloride vapor produced in a bath kept at 363 K was carried in a stream of hydrogen gas at a flow rate of 150 SCCM into the CVD reactor, where pure iron samples were suspended over a pool of molten aluminum at a desired temperature in the range 1173–1373 K. The pressure in the CVD reactor was maintained at 1.33 ± 0.13 kPa. The vapor reacted with the aluminum to produce aluminum subchlorides that were transported to the substrate by gas-phase diffusion and aluminum deposition took place approximately as per reaction (1). At the high temperatures of deposition, aluminum was simultaneously diffused into the substrate to form the aluminide coatings.

2.1. Rate of transport of aluminum to the substrate by gas-phase diffusion

2.1.1. Partial pressures of aluminum subchlorides at the temperature of deposition

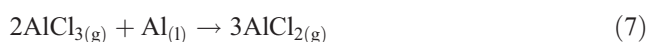
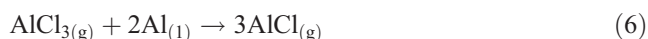
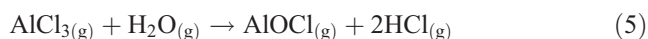
Chemical vapor deposition of aluminide coatings on iron involves the following steps in addition to those of the pack cementation mentioned in the beginning.

1. Heating anhydrous AlCl_3 at a known temperature to produce the vapor.

2. Transport of AlCl_3 vapors to the CVD reactor in a stream of hydrogen gas.

The partial pressure of AlCl_3 in the CVD reactor depends to a first approximation on the AlCl_3 bath temperature. However, since the AlCl_3 vapor is carried in a stream of hydrogen, the partial pressure of AlCl_3 also depends on the flow rate [18]. It was shown that under the experimental conditions used here, the carrier gas would be $\sim 90\%$ saturated with $\text{AlCl}_{3(g)}$ [19]. The partial pressures of the subchlorides of aluminum in the temperature range, 1173 K–1373 K in equilibrium with pure aluminum and 11 compositions of Fe–Al alloys (the coatings) were calculated using a thermodynamic package ‘SOLGASMIX’ [20]. The program is based on the fundamental principle of chemical thermodynamics that the Gibb’s free energy of a system at constant temperature and pressure decreases during an irreversible process and reaches a minimum at the equilibrium state. The output is the partial pressure of various species at the point of minimum free energy. It has the ability to calculate the equilibrium compositions of all the gaseous species and condensed species at constant temperature and pressure (total pressure). The input parameters are the number of moles of H_2 , O_2 and AlCl_3 at various temperatures in the CVD reactor and the standard free energy of formation of various species as a function of temperature.

The incoming gas contained H_2 at 1.33 kPa and AlCl_3 at 90 % of the saturated vapor pressure at the bath temperature (363 K). In addition to these, it contained oxygen due to leakage. It was estimated that the maximum oxygen partial pressure in the LPCVD reactor by leakage would be ≈ 0.013 kPa. When this system was heated to the coating temperature, it produced a complex mixture of gases and solids at equilibrium. The following chemical reactions were considered.



The partial pressure of various species at the coating-vapor interface can be calculated by assuming that the same gases react with the Fe–Al alloys of composition equal to that of the coating. The reaction in this case will be controlled by the activity of aluminum in the Fe–Al alloy present at the surface. Reaction (5) is the source of HCl in the CVD

reactor, which can be minimized if good vacuum is maintained. Some researchers consider the reduction of the monochloride of aluminum with hydrogen as a possible mechanism of deposition [21]. However, thermodynamic calculation showed that it would not have any significant contribution due to the unfavorable free energy.

A small volume of the reactor (cell), containing the sample, was selected for the thermodynamic calculation, where equilibrium was assumed to exist. The number of moles of various species in this volume was calculated assuming ideal gas behavior. The free energy data for the various chemical species formed in the CVD reactor at the temperature of deposition were obtained from 'JANAF Thermo-chemical tables' [22]. For all condensed phases, the standard state was taken to be the pure solid and for all gaseous species, the standard state was taken to be the pure gas at 101.325 kPa (one atmospheric pressure).

The activity of aluminum in different Fe–Al alloys required for calculating the equilibrium concentrations of aluminum subchlorides and other species in equilibrium with the aluminide substrate were available in the literature [23]. Table 1 shows the partial pressure of various species in the reactor at 1173 K in equilibrium with pure aluminum. The total pressure was 1.33 kPa and the AlCl_3 partial pressure was 0.0415 kPa. Similar output tables were obtained with the input gas in equilibrium with pure aluminum and 11 compositions of Fe–Al alloys at five different temperatures in 60 output tables.

The effect of oxygen leak rate on the partial pressure of the aluminum subchlorides was studied. SOLGASMIX calculations were done with oxygen partial pressures 0.0013, 0.013, 0.13 and 0.665 kPa in the reactor. The results showed that the partial pressure of the subchlorides was exactly the same in all these cases. The only difference was

Table 1

The partial pressure of various species in the CVD reactor at 1173 K in equilibrium with pure aluminum, calculated using the thermodynamic package SOLGASMIX [20]

Species	Partial pressure (kPa)
$\text{H}_{2(g)}$	1.2070
$\text{O}_{2(g)}$	0.19428×10^{-36}
$\text{Cl}_{2(g)}$	0.64575×10^{-17}
$\text{HCl}_{(g)}$	0.1350×10^{-3}
$\text{H}_2\text{O}_{(g)}$	0.73922×10^{-11}
$\text{AlCl}_{(g)}$	0.10894
$\text{AlCl}_{2(g)}$	0.79073×10^{-3}
$\text{AlCl}_{3(g)}$	0.423589×10^{-3}
$\text{Al}_2\text{Cl}_{6(g)}$	0.23548×10^{-10}
$\text{AlOCl}_{(g)}$	0.5677×10^{-11}
$\alpha\text{-Al}_2\text{O}_{3(s)}$	0.72933×10^{-7} moles

The total pressure was 1.33 kPa and the AlCl_3 partial pressure was 0.0415 kPa. The amount of solid product $\alpha\text{-Al}_2\text{O}_3$ is reported on the last line (moles).

Note: The software calculates the partial pressures by the free energy minimization technique. The partial pressure (composition) of various species corresponding to the minimum Gibb's free energy of the system is the equilibrium partial pressure (composition).

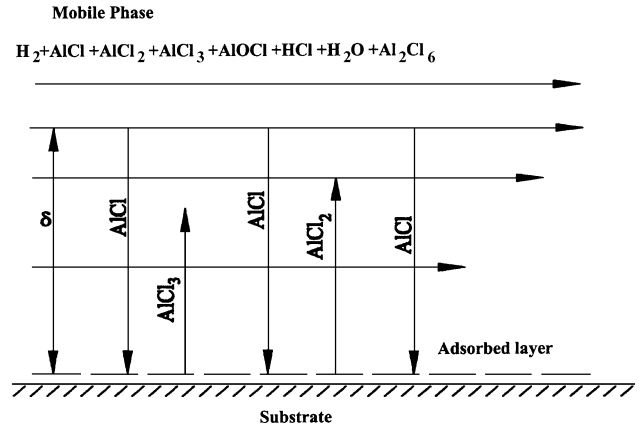


Fig. 1. Schematic diagram of the diffusion layer in CVD aluminide coating.

the quantity of aluminum oxide produced in each case. The mass of aluminum oxide increased with increase in the oxygen partial pressure in the system.

2.1.2. Transport of the aluminum subchlorides to the substrate

A schematic diagram of the diffusion layer in CVD aluminide coating is shown in Fig. 1. There will be a stationary layer of carrier gas adsorbed to the surface of the substrate. Aluminum chlorides in this layer is in equilibrium with the coating. Adjacent to that there are several layers of carrier gas flowing at speeds progressively increasing to the bulk carrier gas velocity at a distance δ cm from the surface. Concentration of vapors in the layers beyond this distance is assumed to be in equilibrium with aluminum source. Using the Fick's law of diffusion and the ideal gas equation, it can be shown that the total flux in milligrams per square centimeter due to all the n aluminum bearing species can be given by the expression [1,19],

$$\frac{dW}{dt} = \frac{1000M}{RT\delta} \sum_{i=1}^n D_i [p_i - p'_i] \text{ mg cm}^{-2}\text{s}^{-1} \quad (9)$$

where dW is the mass of aluminum bearing species transported in time dt (mg).

D_i	is the diffusion coefficient of the i th species ($\text{cm}^2 \text{s}^{-1}$)
δ	is the diffusion layer thickness (cm)
R	is the gas constant ($\text{cm}^3 \text{atm deg}^{-1} \text{mol}^{-1}$)
p_i	is the partial pressure of the i th species in equilibrium with pure aluminum (atm) and
p'_i	is the partial pressure of the i th species in equilibrium with the substrate (atm)

The aluminum-bearing species are in equilibrium with pure aluminum in the bulk phase and with Fe–Al alloy coating at the coating-vapor interface. If a small amount of a species is transported from the bulk to the coating-vapor interface the equilibrium will not be disturbed and the

excess concentration will be converted to the condensed phase, as Fe–Al alloy. This means that the flux of aluminum subchlorides will be the flux of the aluminum from the bulk to the coating substrate. Unlike in pack cementation, in CVD, the diffusion layer thickness cannot be expressed as a simple function of experimental parameters. However, it is a constant determined by fluid dynamics in the reactor. Calculation of the diffusion layer thickness is very complex and hence, in this study, to start with, it was assumed that $\delta=1$ cm. By integrating the expression with respect to time we get a linear relationship between the mass of aluminum transported W and time t in contrast to a parabolic expression for pack cementation [1]. The rate constant for the transport of aluminum by gas-phase diffusion can then be given by the expression:

$$k_g = \frac{27,000}{82.5T\delta} [D_{\text{AlCl}}(p - p')_{\text{AlCl}} + D_{\text{AlCl}_2}(p - p')_{\text{AlCl}_2} + D_{\text{AlCl}_3}(p - p')_{\text{AlCl}_3} + 2D_{\text{Al}_2\text{Cl}_6}(p - p')_{\text{Al}_2\text{Cl}_6} + D_{\text{AlOCl}}(p - p')] \text{ mg cm}^{-2} \text{ s}^{-1} \quad (10)$$

The diffusion coefficients (D) of various halide species were taken from the literature [1]. The D values at the temperatures of interest in this study were obtained from the regression equation obtained by the linear fit of $\log D$ versus $1/T$ (K) of these data. Whenever the D values were not available, they were calculated using the equation.

$$\frac{D_1}{D_2} = \sqrt{\frac{M_2}{M_1}} \quad (11)$$

where D_1 and D_2 are diffusion coefficients of two species of molecular weight M_1 and M_2 , respectively. In LPCVD, the diffusion coefficients are substantially higher than those that exist in pack cementation, due to the reduced pressure. The diffusion coefficients at low pressure were calculated using the relation,

$$D_1 = D_2 \frac{p_2}{p_1} \quad (12)$$

where D_1 and D_2 are the diffusion coefficients at pressures p_1 and p_2 , respectively [1]. The diffusion coefficients of various species used in this study are tabulated in Table 2. They were used for calculating the rate constant for the transport of aluminum to Fe–Al alloy coatings of surface composition varying from 10 to 75 at.% Al at different substrate temperatures. The AlCl_3 bath temperature was fixed at 363 K. Fig. 2 shows the plot of rate constant for vapor transport, k_g , as a function of surface composition. The horizontal portions of the curve show two-phase regions where the aluminum activity does not change.

Table 2

Diffusion coefficients of various gaseous species used in this study ($\text{cm}^2 \text{ s}^{-1}$) calculated from Ref. [1]

Temperature (K)	Diffusion coefficients ($\text{cm}^2 \text{ s}^{-1}$) at 1.33 kPa				
	$\text{AlCl}_{(\text{g})}$	$\text{AlCl}_{2(\text{g})}$	$\text{AlCl}_{3(\text{g})}$	$\text{Al}_2\text{Cl}_{6(\text{g})}$	$\text{AlOCl}_{(\text{g})}$
1173	75.9	59.6	50.2	35.5	60.3
1223	81.3	63.8	53.8	38.0	64.7
1273	86.8	68.0	57.4	40.6	69.0
1323	92.1	72.0	60.9	43.0	73.2
1373	97.3	76.0	64.3	45.5	77.4

The diffusion coefficients at a different temperature were obtained from the linear fit; $\log D$ versus $(1/T)$ (K). The diffusion coefficients at low pressure were calculated using the reciprocal relationship of diffusion coefficient and pressure (see text).

2.2. Rate of diffusion of aluminum from the surface into the substrate

The mass of aluminum diffused into the substrate in time, t can be calculated from the aluminum concentration profile at that instant, which can be obtained from Fick's second law of diffusion. Solution of the diffusion equation is simple only when a single phase is involved and the diffusion coefficient does not vary with concentration. In the case of Fe–Al system, there are several intermetallic phases, and the equation is applicable to each phase. A complete solution across multiple phase fields is available elsewhere [11]. However, in our CVD experiments, in almost all cases, the coatings consist of FeAl phase with aluminum concentration less than or equal to 52 at.% Al [19]. In this composition range, although the interdiffusion coefficient (chemical diffusion coefficient) changes with composition, the change is small and can be assumed to be constant without introducing significant error in the results [12,13]. The average interdiffusion coefficient D_x of Fe–Al alloys below 52 at.% Al and in the temperature range 1073–1473 K can be expressed by the equation [12,13]:

$$D_x = 72.9 \exp\left(\frac{-29,000}{T}\right) \text{ cm}^2 \text{ s}^{-1} \quad (13)$$

With these assumptions, the diffusion equation was solved and the concentration profile was obtained [12,13]. The rate constant can be obtained by integrating the concentration profile as a function of diffusion distance over a period of time and is given by the expression [12,13],

$$k_s = \frac{4D_x C_s^2}{\pi} \text{ mg}^2 \text{ cm}^{-4} \text{ s}^{-1} \quad (14)$$

where k_s is the parabolic rate constant for aluminum transport in the solid phase, C_s is the surface concentration ($\text{mg} (\text{cm}^3)^{-1}$), D_x is the diffusion coefficient ($\text{cm}^2 \text{ s}^{-1}$).

Composition, C_s (mg/cm^3) of the alloy was obtained from the relationship

$$C_s (\text{mg of Al}/\text{cm}^3) = \frac{27,000dC}{[27C + (100 - C)57.8]} \quad (15)$$

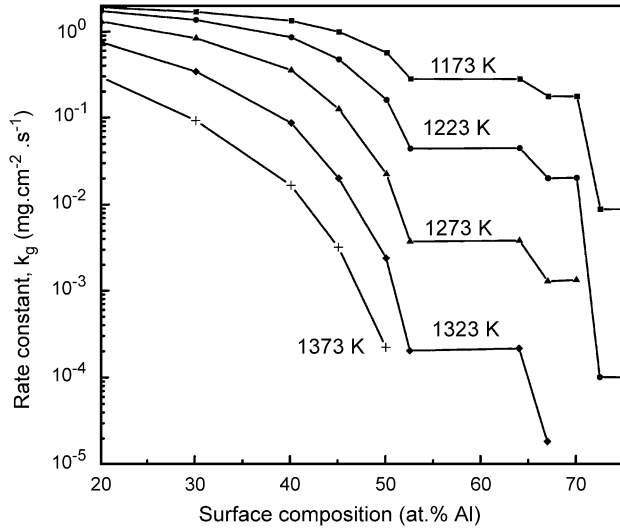


Fig. 2. Rate constant k_g for transport of aluminum chlorides to the surface of the substrate as a function of surface composition at different temperatures.

where d is the density ($\text{gm}(\text{cm}^3)^{-1}$) of the alloy at composition C (at.% Al). The alloy density d can be obtained as a function of alloy composition C (at.% Al) from the polynomial fit of the density-composition data [24], as given by

$$d = 7.87989 - 0.0622056C + 7.08382 \times 10^{-4}C^2 - 7.42992 \times 10^{-6}C^3 \quad (16)$$

Fig. 3 shows the plot of k_s versus concentration of aluminum at the surface in atom percent at different temperatures for the diffusion of aluminum from the surface to interior. The horizontal section in the graph corresponds to the two-phase region where the aluminum activity does not change with composition.

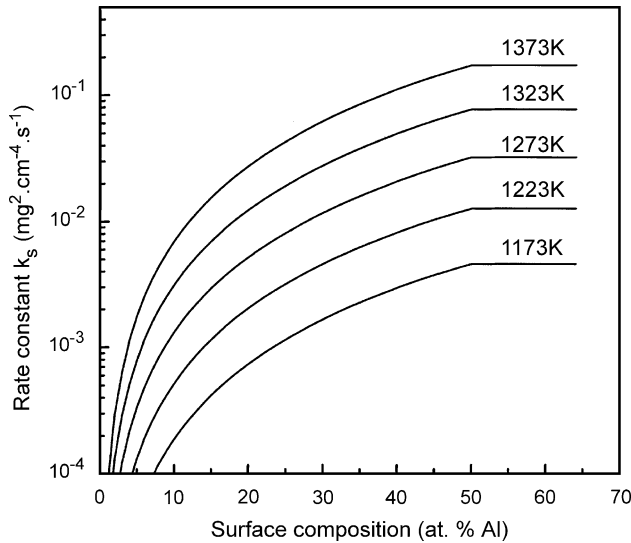


Fig. 3. The rate constant k_s for diffusion of aluminum in the Fe–Al system as a function of surface composition at different temperatures.

3. Discussion

Figs. 4 and 5 show the plot of k_s and $k_g^2 t$ versus surface composition of the coating [14] at 1173 and 1223 K, respectively. In Fig. 4, the point of intersection of the graphs gives surface concentration of aluminum as 71.5 at.% and the rate constant of formation as $0.041 \text{ mg}^2 \text{ cm}^{-4} \text{ s}^{-1}$. In Fig. 5, the point of intersection of the graphs gives the surface concentration of aluminum as 66.9 at.% and the rate constant of coating formation as $0.022 \text{ mg}^2 \text{ cm}^{-4} \text{ s}^{-1}$. The experimentally measured surface concentration and rate constant are 52 at.% Al and $0.0047 \text{ mg}^2 \text{ cm}^{-4} \text{ s}^{-1}$, respectively, at 1173 K and 52 at.% Al and $0.014 \text{ mg}^2 \text{ cm}^{-4} \text{ s}^{-1}$ at 1223 K. In both the cases, the surface composition of the coating and the rate of deposition at the point of intersection does not match with the experimental data because the rate of transport of aluminum to the substrate by vapor phase diffusion takes place at a much higher rate than the rate of solid phase diffusion. In fact, the rate of transport of aluminum to the substrate may be occurring at a faster rate than that is predicted by this graph (the gas transport curve will be shifted to higher side) because in these calculations, the diffusion layer thickness δ is arbitrarily fixed as 1 cm. According to Pierson [25], the boundary layer (diffusion layer) thickness in CVD reactors at very low pressures is negligibly small. Under low pressures, high temperatures and high carrier gas velocities [20–24 cm/s in this case], the diffusion layer thickness will be extremely small, if not, negligible. This will make the gas transport extremely fast compared to the solid phase diffusion in the coatings. Hence, the transport of aluminum bearing species to the substrate will cease to be a rate-limiting step in the kinetics of formation of CVD coatings at low pressures. It may be stressed that although aluminum transport to the surface is

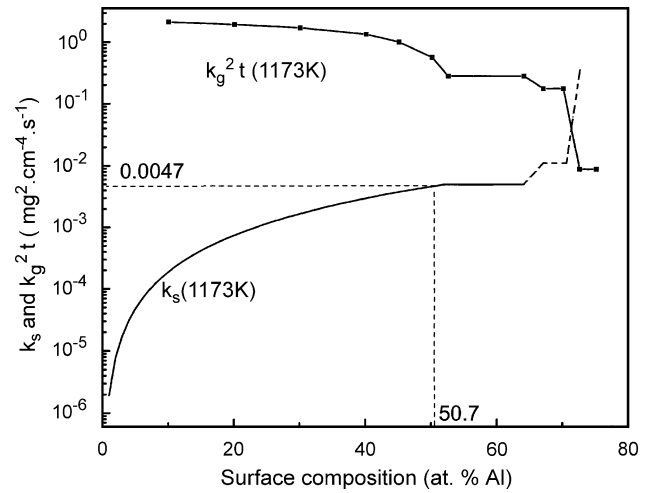


Fig. 4. Plot of the rate constant k_s and $k_g^2 t$ at 1173 K as a function of surface composition. The model for LPCVD (dotted lines) predicts surface composition of the coating corresponding to the experimentally determined rate constant. The portion of the k_s curve above 64 at.% Al is only a rough estimate based on Ref. [13].

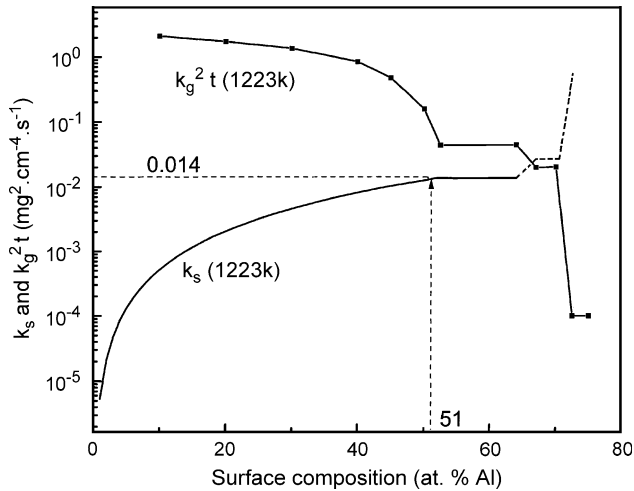


Fig. 5. The plot of the rate constant k_s and $k_g^2 t$ at 1223 K as a function of surface composition. The model for LPCVD (dotted lines) predicts surface composition of the coating corresponding to the experimentally determined rate constant. The portion of the k_s curve above 64 at.% Al is only a rough estimate based on Ref. [13].

very fast compared to solid-state diffusion, it cannot deposit aluminum at the substrate to such an extent as to allow the aluminum activity to reach unity as the rate of transport of aluminum is decided by the difference in the activity of aluminum of the source alloy and the coating surface. When the aluminum concentration at the surface increases above the steady state concentration determined by the diffusion inside the solid, the rate of transport decreases. Hence, pure aluminum is never observed on CVD aluminide coatings unlike in the case of hot dip coatings.

Under this condition, the rate of solid phase diffusion decides the kinetics of formation of the coatings and the surface composition. In fact, experimental studies showed that the coating growth followed parabolic kinetics [17], which is characteristic of solid phase diffusion controlled processes. Hence, for LPCVD, the gas–solid diffusion model applied to pack cementation and APCVD has to be modified. The surface composition of the coating can be

Table 3
Comparison of the experimental results and the surface composition predicted by the model for LPCVD

Substrate temperature T (K)	Result from experimental study		Coating composition (at.% Al) predicted from the model corresponding to k_p
	Parabolic rate constant k_p [17]	Coating composition (at.% Al)	
1173	0.0047	52.0	50.7
1223	0.014	52.0	51.0
1280	0.035	49.5	49.7
1323	0.063	46.2	46.4
1373	0.13	44.6	42.6

Column 2 gives the experimentally determined growth rate constants (k_p) and the surface composition of the corresponding coatings. Column 3 shows the surface composition of the coatings predicted using the model, using the experimentally determined rate constants, k_p [17].

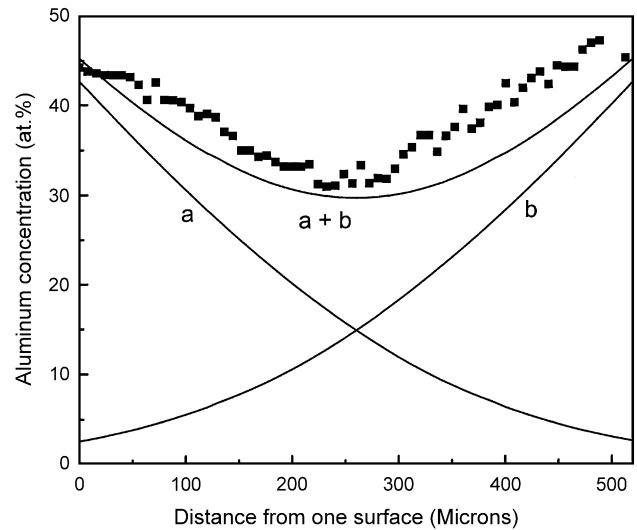


Fig. 6. Concentration profile of aluminum predicted by the model (continuous line) is superimposed over the concentration profile of the coating produced at 1373 K determined experimentally by EPMA (black dots).

obtained from the k_s versus C_s curve and the experimentally determined rate of deposition as shown by the dotted lines in Figs. 4 and 5. The surface composition obtained from the model and the experimentally obtained surface composition are given in Table 3. An excellent agreement is seen between the experimental and calculated values.

In pack cementation and APCVD, the point of intersection of the plots of the rate of transport of aluminum to the substrate by gas-phase diffusion and that from the surface into the substrate by solid phase diffusion as a function of surface composition gives both surface composition of the coating as well as the rate of coating formation. In LPCVD,

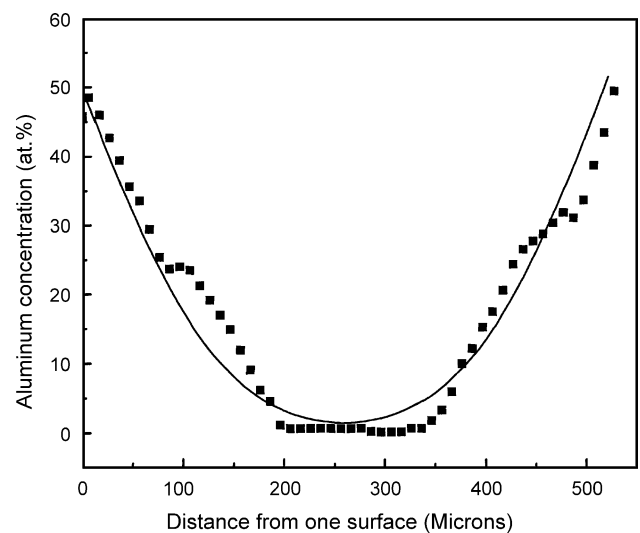


Fig. 7. Concentration profile of aluminum predicted by the model (continuous line) is superimposed over the concentration profile of the coating produced at 1273 K determined experimentally by EPMA (black dots).

since the rate of transport of aluminum by gas-phase diffusion is very fast, it does not contribute to the kinetics of the process. The process is modeled based on the rate of solid phase diffusion. Hence, with this model for LPCVD, if we know either the surface composition or the rate of formation, the other variable can be determined.

The concentration profile of aluminum along the cross-section of the coating calculated by using the surface concentration predicted by the model for a deposition with a substrate temperature of 1373 K and AlCl_3 bath temperature of 363 K is shown in Fig. 6. The concentration profile, measured by electron probe micro-analyzer (EPMA) on the corresponding sample is superimposed in this figure. Fig. 7 shows the corresponding data for a sample deposited at 1273 K and AlCl_3 bath temperature of 363 K. Since coating was done on both sides of the sample, the aluminum concentration profile across the thickness of the sample was obtained by adding the concentration profiles of both sides. Since the sample was only 0.5 mm thick, aluminum diffusing from opposite sides merged at the center in the case of sample produced at 1373 K. Concentration profile of aluminum from the two sides is marked 'a' and 'b' in Fig. 6. The resultant composition is given by the sum of the individual profiles. There is excellent correlation between the concentration profile calculated from the model and the aluminum profile obtained by EPMA in samples produced experimentally.

4. Conclusion

The dual diffusion model successfully applied to aluminum coating by pack cementation and APCVD needs to be modified for applying to the LPCVD process. For the latter, the rate of vapor transport is much higher than that of the solid-state diffusion due to the increase in diffusion coefficient and reduction of diffusion layer thickness at low pressures. Hence, the kinetics of deposition in LPCVD is controlled by the solid-state diffusion. The surface composition of the coatings can be obtained from the plot of the rate of solid-phase diffusion versus surface composition. The surface composition values obtained from the model matched well with the surface composition of the samples

measured experimentally. The overall growth kinetics was consistent with this model.

References

- [1] S.R. Levine, R.M. Caves, *J. Electrochem. Soc.* 121 (1974) 1051.
- [2] J. Hickl, R.W. Heckel, *Metall. Trans., A, Phys. Metall. Mater. Sci.* 6A (1975) 431.
- [3] R.W. Heckel, M. Yamada, C. Ouchi, A.J. Hickl, *Thin Solid Films* 45 (1977) 367.
- [4] A.K. Sarkhel, L.L. Seigle, *Metall. Trans., A, Phys. Metall. Mater. Sci.* 7A (1976) 899.
- [5] B.K. Gupta, A.K. Sarkhel, L.L. Seigle, *Thin Solid Films* 39 (1976) 313.
- [6] R. Sivakumar, L.L. Seigle, *Metall. Trans., A, Phys. Metall. Mater. Sci.* 7A (1976) 1073.
- [7] B.K. Gupta, L.L. Seigle, *Thin Solid Films* 73 (1980) 365.
- [8] N. Kandasamy, L.L. Seigle, F.J. Pennisi, *Thin Solid Films* 84 (1981) 17.
- [9] S.K. Gupta, S.R. Adolph, L.C. Tandon, L.L. Seigle, *Metall. Trans., A, Phys. Metall. Mater. Sci.* 13A (1982) 495.
- [10] T.H. Wang, L.L. Seigle, *Mater. Sci. Eng., A Struct. Mater.: Prop. Microstruct. Process.* 108 (1989) 253.
- [11] B. Nciri, L. Vandenbulke, *Surf. Technol.* 24 (1985) 365.
- [12] B. Nciri, L. Vandenbulke, *J. Less-Comm. Met.* 95 (1983) 191.
- [13] B. Nciri, L. Vandenbulke, *Thin Solid Films* 139 (1986) 311.
- [14] W.P. Sun, H.J. Lin, M.H. Hon, *Thin Solid Films* 146 (1987) 55.
- [15] H.J. Lin, W.P. Sun, M.H. Hon, *Thin Solid Films* 156 (1988) 259.
- [16] W.P. Sun, H.J. Lin, M.H. Hon, *Metall. Trans., A, Phys. Metall. Mater. Sci.* 17A (1986) 225.
- [17] J.T. John, R.S. Srinivasa, P.K. De, *Thin Solid Films* (doi: 10.1016/j.tsf.2004.02.042).
- [18] U. Merten, W.E. Bell, in: J.L. Margrave (Ed.), *Characterization of High Temperature Vapors*, Wiley, New York, 1967, p. 95.
- [19] J.T. John, PhD thesis, Indian Institute of Technology, Bombay, India (2001).
- [20] G. Erikson, *Chem. Scr.* 8 (1975) 100.
- [21] N. Voudouris, Ch. Christoglou, G.N. Angelopoulos, *Surf. Coat. Technol.* 141 (2001) 275.
- [22] M.W. Chase Jr., C.A. Davies, J.R. Downey Jr., D.J. Frurip, R.A. McDonald, A.N. Syverud (Eds.), *JANAF Thermochemical Tables, Part I, Third Edition*, Am. Chem. Soc. and Am. Inst. Phys. for Natl. Bureau of Standards, Michigan, USA, 1985.
- [23] J. Eldridge, K.L. Komarek, *Trans. Met. Soc. AIME* 230 (1964) 226.
- [24] J.H. Schneibel, in: J.H. Schneibel, M.A. Crimp (Eds.), *Processing, Properties and Application of Iron Aluminides, Minerals, Metals & Materials Society*, Pennsylvania, 1994, p. 329.
- [25] H.O. Pierson, *Hand book of Chemical Vapor Deposition*, Noyes Publications, New Jersey, 1992, p. 17.